Imatinib- and ponatinib-mediated cardiotoxicity in zebrafish embryos and H9c2 cardiomyoblasts

ZAIN Z. ZAKARIA[1], MUNA SULEIMAN[2], FATIHA M. BENSLIMANE[3], MASHAEL AL-BADR[4,5], SIVEEN SIVARAMAN[6], HESHAM M. KORASHY[2], FAREED AHMAD[7], SHAHAB UDDIN[7,8], FATIMA MRAICHE[2,9] and HUSEYIN C. YALCIN[3]

[1]Vice President of Health and Medical Sciences Office, QU Health, Qatar University, Doha 2713, Qatar; [2]Department of Pharmaceutical Sciences, College of Pharmacy, QU Health, Qatar University, Doha 2713, Qatar; [3]Biomedical Research Center, Qatar University, Doha 2713, Qatar; [4]Department of Biology, College of Art and Science, Qatar University, Doha 2713, Qatar; [5]National Reference Laboratory, Ministry of Public Health, Doha 7744, Qatar; [6]Translational Research Institute, Hamad Medical Corporation, Doha 3050, Qatar; [7]Translational Research Institute and Dermatology Institute, Hamad Medical Corporation, Doha 3050, Qatar; [8]Laboratory Animal Research Center, Qatar University, Doha 2713, Qatar

Received August 4, 2023; Accepted April 26, 2024

DOI: 10.3892/mmr.2024.13311

Abstract. Tyrosine kinase inhibitors (TKIs) offer targeted therapy for cancers but can cause severe cardiotoxicities. Determining their dose-dependent impact on cardiac function is required to optimize therapy and minimize adverse effects. The dose-dependent cardiotoxic effects of two TKIs, imatinib and ponatinib, were assessed *in vitro* using H9c2 cardiomyoblasts and *in vivo* using zebrafish embryos. *In vitro*, H9c2 cardiomyocyte viability, apoptosis, size, and surface area were evaluated to assess the impact on cellular health. *In vivo*, zebrafish embryos were analyzed for heart rate, blood flow velocity, and morphological malformations to determine functional and structural changes. Additionally, reverse transcription-quantitative PCR (RT-qPCR) was employed to measure the gene expression of atrial natriuretic peptide (ANP) and brain natriuretic peptide (BNP), established markers of cardiac injury. This comprehensive approach, utilizing both *in vitro* and *in vivo* models alongside functional and molecular analyses, provides a robust assessment of the potential cardiotoxic effects. TKI exposure decreased viability and surface area in H9c2 cells in a dose-dependent manner. Similarly, zebrafish embryos exposed to TKIs exhibited dose-dependent heart malformation. Both TKIs upregulated ANP and BNP expression, indicating heart injury. The present study demonstrated dose-dependent cardiotoxic effects of imatinib and ponatinib in H9c2 cells and zebrafish models. These findings emphasize the importance of tailoring TKI dosage to minimize cardiac risks while maintaining therapeutic efficacy. Future research should explore the underlying mechanisms and potential mitigation strategies of TKI-induced cardiotoxicities.

Correspondence to: Dr Huseyin C. Yalcin, Biomedical Research Center, Qatar University, Al Dafna, 233 Al Jamia Street, Doha 2713, Qatar
E-mail: hyalcin@qu.edu.qa

Dr Fatima Mraiche, Department of Pharmaceutical Sciences, College of Pharmacy, QU Health, Qatar University, Al Dafna, 309 Al Jamia Street, Doha 2713, Qatar
E-mail: fmraiche@qu.edu.qa

Present address: [9]Department of Pharmacology, Faculty of Medicine & Dentistry, College of Health Sciences, Edmonton, AB T6G 2H7, Canada

Key words: zebrafish, H9c2 cardiomyoblast, cardiac function, tyrosine kinase inhibitor, imatinib, ponatinib, blood flow, shear stress

Introduction

Chronic myeloid leukemia (CML) is a prevalent form of leukemia, accounting for ~15% of all leukemia diagnoses and posing a significant global health burden (1,2). The discovery of dysregulated tyrosine kinase (TK) activity in CML pathogenesis facilitated development of TK inhibitors (TKIs) as a targeted therapy (3). This approach has improved the prognosis of patients with CML, achieving long-term remission rates >80% (3). Despite these advances, challenges remain in optimizing TKI treatment and understanding the long-term effects. The present study aimed to assess the dose-dependent impact of TKI on cardiac function to optimize therapy and minimize adverse effects. A deeper understanding of the mechanisms underlying TKI action in CML is key for developing patient-specific treatment regimens that balance anticancer effects with the prevention or mitigation of cardiotoxic side effects.

TKs are a group of enzymes within the protein kinase family. They act as molecular switches, regulating cellular processes such as proliferation, differentiation, metabolism and apoptosis by attaching phosphate groups from ATP to specific proteins (4). This phosphorylation can either activate

or inhibit the target protein. Dysregulation of TKs serves a key role in cancer development and progression (4). Studies have identified ~58 different TK receptors associated with numerous cancers (5-7). When activated in cancer cells, TKs promote tumor growth by stimulating cell proliferation, angiogenesis, resistance to cell death and metastasis (8). Therefore, understanding the specific roles of TKs in different cancer types is essential for developing targeted therapeutic strategies. By inhibiting these aberrantly active kinases, key cancer-promoting pathways can be disrupted, offering potentially more effective treatment options. TKIs have emerged as a drug against numerous types of cancers, including CML (9,10). TKIs are classified into generations based on their specificity and affinity for certain TKs, reflecting the progression in TKI development aimed at optimizing therapeutic effectiveness while minimizing side effects for patients. First-generation TKIs like imatinib, sunitinib, and gefitinib are pioneering drugs with a broad activity spectrum. They target multiple TKs, including both cancer-causing targets and non-intended kinases. This wide range of activity can lead to effective initial tumor reduction but also increases the likelihood of side effects from inhibiting non-target essential cellular processes. In contrast, second and third-generation TKIs, such as dasatinib and ponatinib, show advancements in design towards greater target specificity. These newer TKIs aim to inhibit only the cancer-causing tyrosine kinases, thereby reducing off-target effects and improving patient outcome (11,12). Despite their similar mode of action, which involves blocking the activation of receptor TKs (RTKs) (13,14) TKIs differ in their target specificity, pharmacokinetics and side effect profiles. While they all prevent RTKs from triggering downstream signaling pathways, the precise targeted kinase and drug interactions determine its effectiveness and potential adverse effects. Understanding these differences is required for optimizing TKI therapy. Researchers continuously evaluate tailored approaches that maximize efficacy while minimizing side effects, leading to better patient outcomes (15).

While effective in treating various types of cancers, TKIs pose significant concerns due to their broad-spectrum targeting, leading to diverse toxicities. Among these, cardiotoxicity is a key side effect, impacting patient quality of life and treatment outcomes (16). For example, imatinib, a first-generation TKI, induces left ventricular dysfunction in patients and preclinical models (17,18). Second-generation TKIs) like dasatinib demonstrate improved selectivity for BCR-ABL proteins. These BCR-ABL proteins, with their aberrant tyrosine kinase activity, are critical drivers of chronic myeloid leukemia (CML) and contribute significantly to treatment resistance. However, dasatinib, despite its targeted action, can still induce cardiotoxicities like pulmonary hypertension and heart failure (19,20). Ponatinib, the only TKI for T3151-mutant CML, exhibits strong cardiotoxic effects, including hypertension and heart failure (21,22). While the cardiotoxic potential of imatinib and ponatinib is established, understanding the underlying mechanisms is crucial for developing targeted mitigation strategies. This study addressed this gap by employing a complementary *in vitro* and *in vivo* approach. H9c2 cardiomyocytes were used for individual cell analysis to investigate potential apoptotic and hypertrophic effects, while zebrafish embryos (ZFEs) provided a platform for whole-organism observations and genetic manipulations. This dual approach aimed to gain a deeper understanding of TKI-induced cardiotoxicity mechanisms. We hypothesized that both imatinib and ponatinib induce cardiomyocyte apoptosis and hypertrophy, with ponatinib exhibiting a stronger effect. Ultimately, this research seeks to pave the way for safer and more effective TKI therapies, improving patient outcomes.

Materials and methods

Culture of H9c2 cardiomyoblasts. This study used H9c2 cardiomyoblasts (European Collection of Cell Cultures) derived from BDIX embryonic rat cardiac tissue. Cells were cultured in Dulbecco's Modified Eagle's Medium Ham's F-12 1:1 (DMEM/F-12; Lonza Group, Ltd.) supplemented with 10% w/v fetal bovine serum (FBS) (Gibco-Thermo Fisher Scientific, Inc.) and 1% w/v penicillin-streptomycin. All cultures were maintained at 37˚C in a humidified environment with 5% CO_2 and 95% O_2. H9c2 cardiomyoblasts represent a well-established *in vitro* model that has been previously used to investigate the molecular mechanisms of action of numerous anticancer agents, including TKIs (23-25).

Treatment of H9c2 cardiomyoblasts. H9c2 cardiomyoblasts were treated with imatinib and ponatinib to investigate their cardiotoxic effects. Stock solutions of both drugs (50 mM) were prepared by dissolving in Hybri-Max DMSO (cat. No. D2660; MilliporeSigma). To ensure consistency, the final concentration of DMSO in the culture media was ≤0.5%. H9c2 cells were treated with imatinib and ponatinib at 2.5 and 5.0 μM. The concentrations used in this study were consistent with those used in previous studies (23,24,26-28). Control cells received an equivalent volume of vehicle (0.5% v/v DMSO) only. Following treatment for 24 h at 37˚C, cells were subjected to further experiments.

MTT assay. The viability of H9c2 cardiomyoblasts following treatment with imatinib or ponatinib was evaluated using MTT assay (MilliporeSigma). Briefly, cells were seeded in 48-well plates at a density of $4x10^4$ cells/well and allowed to adhere for 24 h at 37˚C. Medium was replaced with fresh Dulbecco's Modified Eagle's Medium Ham's F-12 1:1 (DMEM/F-12) (Lonza, Basal, Switzerland) supplemented with 10% FBS) and 1% penicillin/streptomycin. Cells were then treated with imatinib or ponatinib at concentrations of 2.5 and 5.0 μM for 24 h at 37˚C. The medium was removed following treatment and 0.5 mg/ml MTT solution was added to each well. Following incubation for 3 h at 37˚C, the resulting formazan crystals were dissolved in DMSO. Absorbance was measured at 570 nm using an Epoch 2 optical microplate reader (Norgen Biotek Corp.). Cell viability was presented as a percentage of vehicle control. To account for non-specific signal, the mean absorbance of blank wells containing medium only was subtracted from all other wells. Background-corrected absorbance values for each treatment group were normalized to the mean absorbance of the vehicle control (0.5% DMSO) to enable cross-group comparisons. Finally, normalized values were multiplied by 100 to present viability as a percentage of the vehicle control. The experiment was repeated three times.

Cell surface area measurement of H9c2 cardiomyoblasts. Cell surface area quantification was performed as previously established (29). Briefly, H9c2 cardiomyoblasts were seeded at a density of 10,000 cells/35-mm culture dish and allowed to adhere for 24 h at 37˚C. Cells were then treated with imatinib or ponatinib at concentrations of 2.5 and 5.0 μM for 24 h at 37˚C. Following treatment, cells were washed with 1X phosphate-buffered saline (PBS), fixed with 4% v/v formaldehyde and stained with 0.5% w/v crystal violet solution for 20 min at room temperature. Stained cells were visualized and captured at 20x magnification using an Axiovert 40 CFL inverted confocal microscope (Carl Zeiss AG). Cell surface area analysis was performed on 15-30 randomly selected cells using AxioVision Imaging software 4.8.2 (Carl Zeiss AG). The experiment was repeated three times. The surface area of the cell was calculated by normalizing the background-corrected absorbance values of each treatment group to the mean absorbance of the vehicle control group (0.5% DMSO) for direct comparison across groups. Then, the normalized values were multiplied by 100 to express the viability of each treatment group as a percentage of the vehicle control.

Flow cytometry analysis of cell death and size of H9c2 cardiomyoblasts. H9c2 cardiomyoblasts were seeded in 35-mm dishes containing DMEM-F12 supplemented with 10% w/v FBS and 1% w/v penicillin-streptomycin. After 24 h 37˚C, they were treated with imatinib or ponatinib at concentrations of 2.5 and 5.0 μM for 24 h at 37˚C. Culture medium was aspirated, and monolayers were rinsed with sterile PBS to remove serum. Cells were detached using 0.25% Trypsin [Gibco-Thermo Fisher Scientific (Waltham, MA, USA)] for ≤10 min at 37˚C, centrifuged (300-400 g, 5 min, at room temperature), and washed with PBS/BSA to remove debris. The final pellet was resuspended in fresh PBS. Cells were stained with annexin-V and propidium iodide (PI) (BD Biosciences) in 1X annexin binding buffer for 30 min at room temperature. Flow cytometry was performed using BD LSRFortessa™ cell analyzer (BD Biosciences) BD FACSDiva software 6.1.3 (BD Biosciences) were used to measure the cell viability. Apoptotic cells were determined as follows: Viable, PI- and annexin-FITC-negative; early stage apoptosis, PI-negative and annexin-FITC-positive; late stage apoptosis PI- and annexin-FITC positive and necrotic, PI-positive and annexin-FITC-negative as previously described (30,31). Cell size was measured with forward light scatter using the flow cytometer and the percentage of cells in early and late apoptosis was calculated as the total proportion of apoptotic cells. The experiment was repeated three times.

ZFEs. Adult zebrafish (AB strain) were maintained in recirculating systems (AQUA NEERING ZD560) at the Qatar University Biomedical Research Center under a 14 h light/10 h dark cycle with controlled temperatures (room: 26˚C, water: 28˚C). All procedures adhered to approved protocols (QU-IACUC, QU-IBC-2022/014) and national/international zebrafish guidelines (27). Standard practices (32) guided breeding. Fish were maintained in reconstituted saltwater tanks and fed twice daily with fresh brine shrimp. For embryo collection, male and female zebrafish were separated overnight using a mesh barrier in a mating tank. The next morning, the barrier was removed, allowing mating for 20 min. Fertilized embryos were collected in freshly prepared E3 medium (32) and staged/fixed according to established protocols (33).

Treatment of ZFE. To assess the cardiac effects of TKIs in a developing organism, fertilized ZFEs were collected and maintained at 28˚C in N-phenylthiourea (PTU) water at a standard concentration of 0.003% (200 μM) to suppress pigmentation and aid observation and time-lapse video acquisition. Experiments used 12-well Falcon Tissue Culture Plate, flat bottom with low evaporation lid (Corning Life Sciences, Netherlands), housing 20 embryos each. For optimal detection of potential toxicity, treatment commenced occurred at 6 h post-fertilization (hpf), corresponding to the 'high stage' as described by Kimmel *et al* (33). This stage is characterized by rapid cell division and organogenesis, rendering the developing embryo highly susceptible to disruptions caused by toxic substances due to the presence of a largely undifferentiated cell population. Following PTU removal, 2 ml drug solution was added. TKI concentrations (2.5, 5.0 and 10.0 μM) were selected based on preliminary tissue culture experiments, ensuring relevance to clinically relevant ranges. The following controls were used: Control, maintained in PTU; negative control, treated with the DMSO vehicle (0.1% v/v) and the positive control (PC), treated with known cardiotoxic agent aristolochic acid I (AA; 1 μM). All drug solutions were prepared in DMSO at a final concentration of 0.1%. Treatment was conducted at 28˚C for 24 h for SR, 48 h for both SR and HR, and 72 h for SR, cardiac function assessment, and cardiac gene assay.

Observation and analysis of ZFEs embryos. At 24-72 hpf, ZFEs were examined every 24 h under a SteREO Discovery V8 light microscope (Carl Zeiss AG) with a Hamamatsu Orca Flash camera (Hamamatsu Photonics UK Limited) and HCImage software 2.0.4 (Hamamatsu Photonics UK Limited) to monitor developmental stage, mortality, hatching, spontaneous movement, response to touch, presence of deformities and heart rate. The phenotypical aberrations were recorded at each point and compared with the controls. Images of the embryos were captured and the number of similar phenotypes in the experimental group noted. Survival and morphological abnormalities were assessed; opaque, coagulated embryos lacking a heartbeat were considered non-viable and removed. The mortality percentage was determined by counting the number of dead ZFEs/group at 24, 48 and 72 hpf divided by the total number of injected embryos x100. Dead embryos were removed at each time point. Potential neurological or muscular defects at 24 hpf were assessed by tail-flicking (burst/min) using Danio Scope software, EthoVision XT9.0 (Noldus Information Technology). The hatching percentage was determined by counting the number of hatched ZFEs/group at 48 and 72 hpf, divided by the total number of injected embryos x100.

Experiments exceeding 20% mortality in the negative control group were excluded. Observed abnormalities were documented. At 72 hpf, six embryos/group were immobilized with 3% methylcellulose at room temperature for 30 sec to conduct cardiovascular analysis. Each embryo underwent 10 sec bright field video recording at 100 frames/sec (fps) of the beating heart and the body. MicroZebralab 3.6 software (Viewpoint)

Table I. Primers used in reverse-transcription quantitative PCR.

Gene	RefSeq	Cat. no.	Assay ID
ANP-nppa zebrafish	NM_198800	4331348	TaqMan Gene Expression Assay ID APGZVJD
BNP-nppa zebrafish	NM_001327776	4331348	TaqMan Gene Expression Assay ID APGZVJD,
B2M	NM_131163.2 NM_001159768.1	4351372	TaqMan Gene Expression Assay Dr03432699_m1

ANP, atrial natriuretic peptide; BNP, Brain Natriuretic Peptide; B2M, Beta-2-Microglobulin.

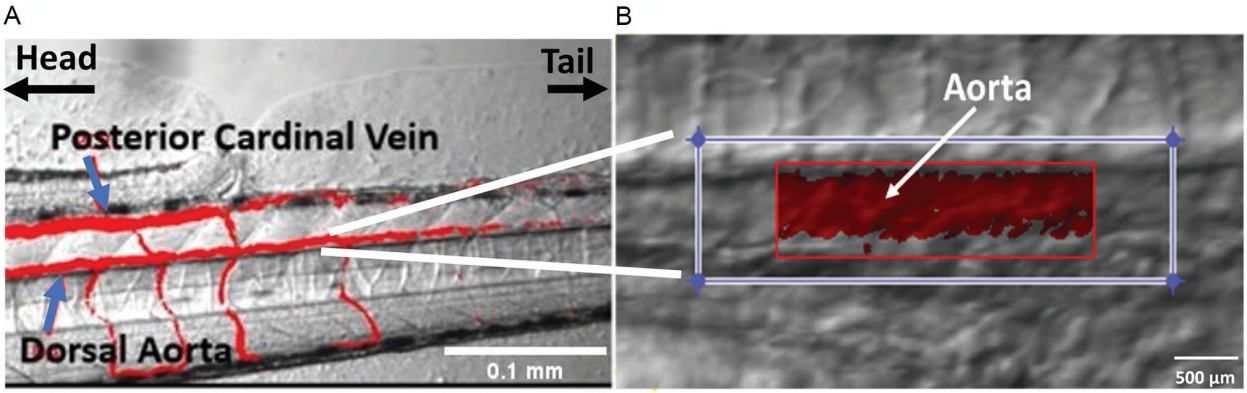

Figure 1. Automated analysis of blood flow in zebrafish embryo. (A) Automated vessel detection using ZebraLab software aided in identifying the DA and PCV. (B) Based on the automated detection, a ROI was defined (dotted line) and validated (red rectangle). The flow of blood cells within the ROI was automatically analyzed. PCV, posterior cardinal vein; DA, dorsal aorta; ROI, region of interest.

was used to determine blood flow velocity, arterial pulse and vessel diameter in the dorsal aorta (DA) and posterior cardinal vein, ensuring consistency across samples (34,35) (Fig. 1).

Cardiac function assessment. The cardiac function of treated and negative control embryos was evaluated at 72 hpf. Time-lapse video capturing beating ventricles and red blood cell (RBC) movement in major vessels was analyzed as described previously (35). An in-house algorithm implemented in Viewpoint ZebraLab software version 3.4.4 (Viewpoint) tracked RBCs, enabling the measurement of aorta blood velocity, heartbeat and aorta diameter (Fig. 1). The mean of these measurements was used to estimate frictional shear stress levels in the cardiovascular system using the formula: Shear stress (τ; dynes/cm^2)=[4 x blood viscosity (dynes/cm^2) x average blood velocity (μm/sec)]/vessel diameter (μm). flow rate (nl/min), was calculated as follows: Average blood velocity (μm/s) x vessel diameter (μm) (34-36).

Gene expression analysis in ZFE. Gene expression changes were detected by reverse transcription-quantitative PCR which involved a 2 min Uracil DNA glycosylase incubation at 50˚C, a 2-min polymerase activation at 95˚C, a 1-sec denaturation at 95˚C, and a final 30-sec annealing at 60˚C. Total RNA was isolated from TKI-treated and negative control embryos using the IBI DNA/RNA/Protein Extraction kit (cat. no. IB47702; IBI Scientific) following the manufacturer's instructions. First-strand cDNA was synthesized from the extracted RNA using the SuperScript™ IV VILO™ Master Mix kit (cat. no. 11756050; Thermo Fisher Scientific, Inc.). Quantitative analysis of specific mRNA expression was performed using TaqMan Fast Advanced Master Mix (Applied Biosystems; Thermo Fisher Scientific, Inc.) and specific primers (Table I) and probes constructed against the genes of interest. These include atrial natriuretic peptide (ANP; Applied Biosystems; Thermo Fisher Scientific, Inc.) and brain natriuretic peptide (BNP; Applied Biosystems, Thermo Fisher Scientific, Inc.). The signal was detected using the ABI 7500 Real-Time PCR System (Applied Biosystems; Thermo Fisher Scientific, Inc.). mRNA levels were quantified using the $2^{-\Delta\Delta Cq}$ method (37) and normalized to the internal reference gene B2M. This approach ensured accurate and consistent gene expression analysis across all samples.

Statistical analysis. Statistical analysis was performed using GraphPad Prism software, version 8 (GraphPad LLC; Dotmatics,). D'Agostino-Pearson normality test confirmed the distribution of parametric data, which were analyzed by one-way ANOVA with Sidak's or Dunnett's post hoc test and two-way mixed ANOVA with either Sidak's or Tukey's post hoc test. $P<0.05$ was considered to indicate a statistically significant difference. All data points are presented as mean ± SEM. Each experiment was performed three times.

Results

Ponatinib induces dose-dependent cytotoxicity in H9c2 cells. To assess the cardiotoxic potential of imatinib and ponatinib, H9c2 cardiomyoblast viability was evaluated using an MTT assay following 24 h treatment. A significant increase in cell

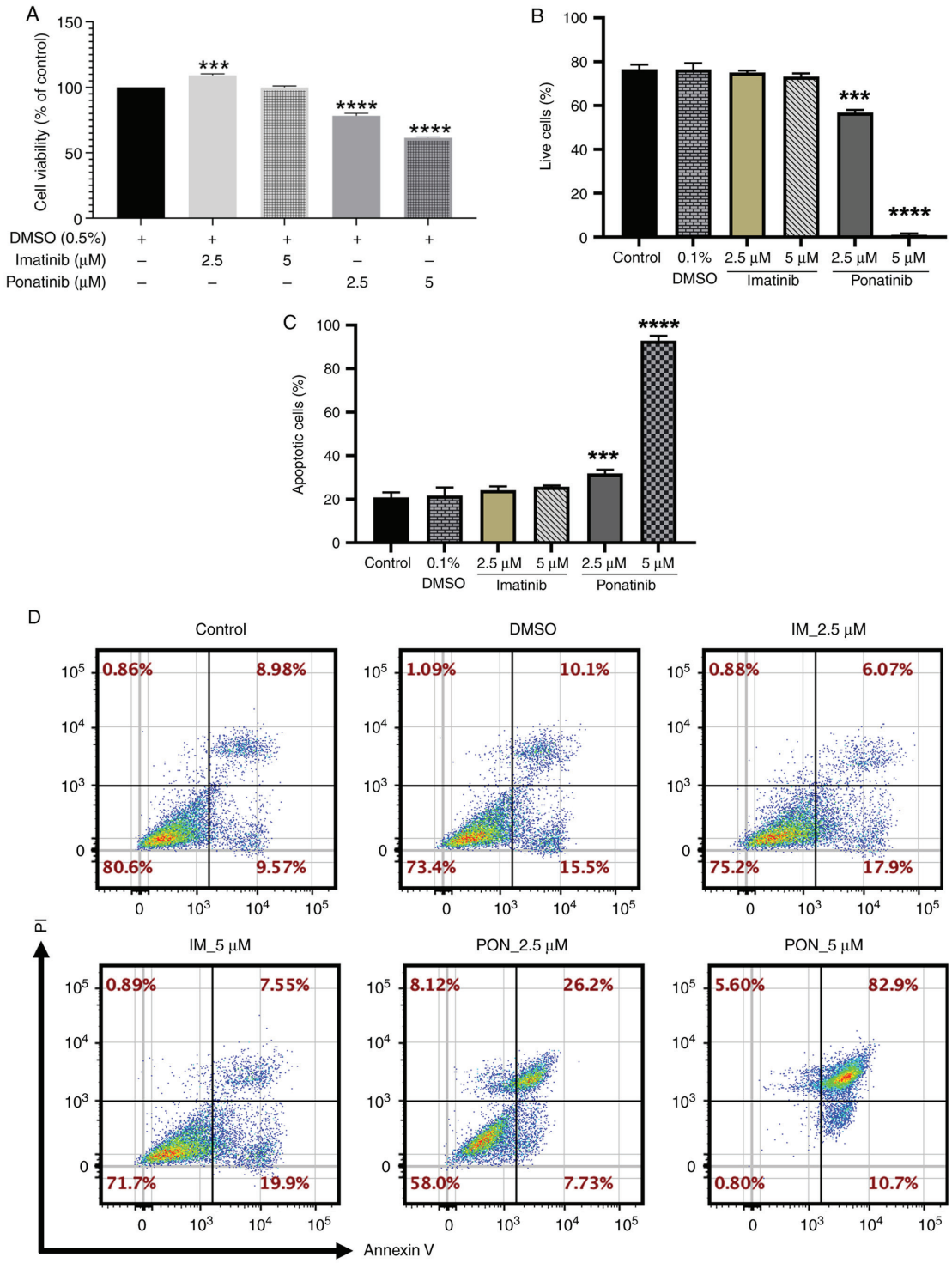

Figure 2. Imatinib and ponatinib induce dose-dependent cytotoxicity in H9c2 cardiomyoblasts. H9c2 cells were treated with imatinib or ponatinib at 2.5 and 5.0 μM for 24 h. (A) Cell viability was assessed by MTT assay and absorbance was measured at 570 nm using an Epoch 2 optical microplate reader. Percentage of (B) viable and (C) apoptotic cells determined using flow cytometry. Values are presented and normalized as a percentage of vehicle negative control (0.5% v/v DMSO). (D) Representative flow cytometry of live, apoptotic and necrotic cells. All data are presented as mean ± SEM (the experiment was repeated three times) (n=3). One-way ANOVA with Dunnett's post hoc test was used to compare groups. ***P<0.001 and ****P<0.0001 vs. DMSO.

viability (109.19±2.35%) compared with the negative control was demonstrated with 2.5 μM imatinib treatment, however, no significant changes were demonstrated at 5 μM. Ponatinib induced significant dose-dependent reductions in cell viability, with a 22% decrease at 2.5 μM (viability, 78.24±3.80%) and a 40% decrease at 5 μM (viability, 61.46±1.49%) compared with the negative control (Fig. 2A).

Flow cytometry confirmed these contrasting effects. While both 2.5 and 5.0 μM ponatinib significantly reduced the number of live cells in the sample population for each group (59.10±2.14 and 6.83±0.07%, respectively) compared with the negative control. Imatinib treatment at each concentration showed no significant change in the number of live cells compared with negative control (Fig. 2B).

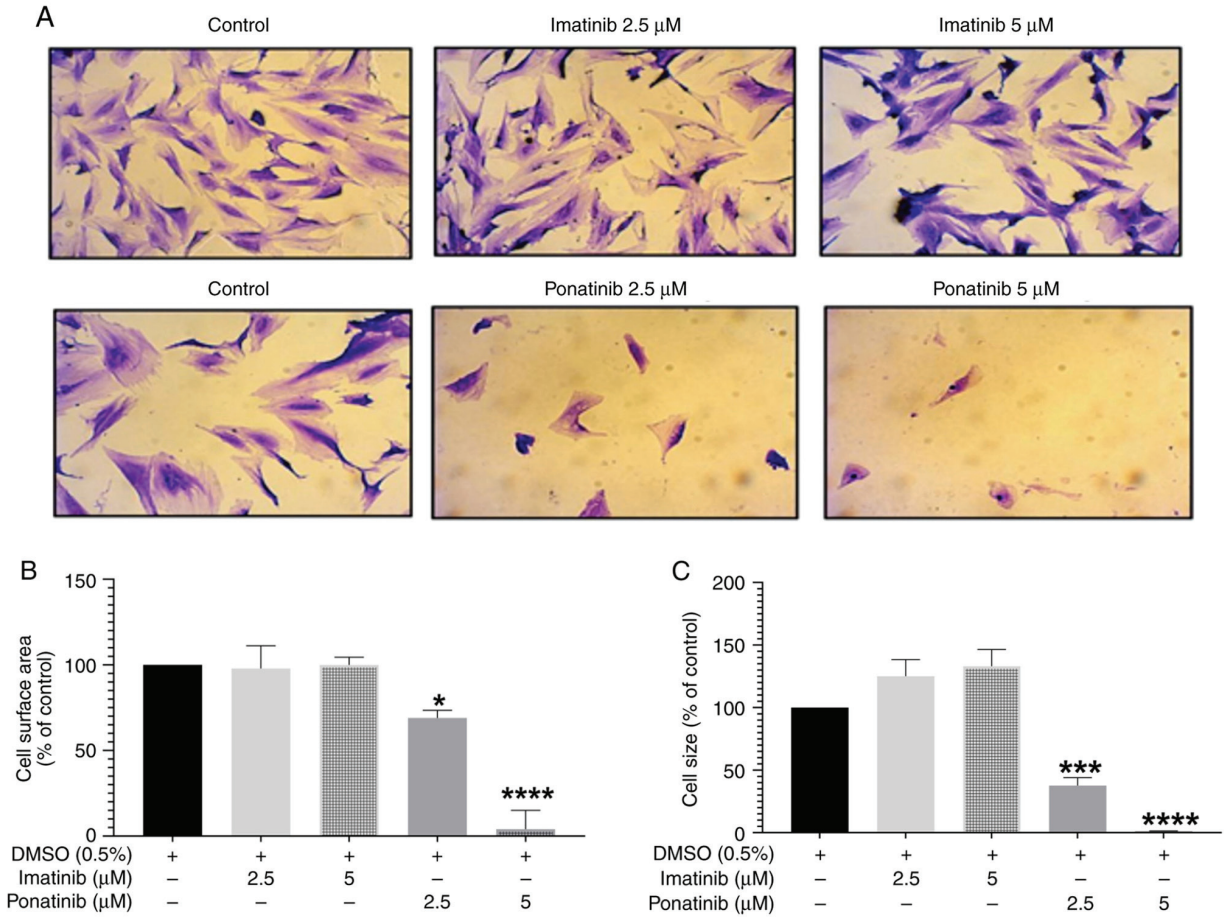

Figure 3. Continued.

To assess the underlying mechanism of cell death, the percentage of apoptotic cells was assessed using flow cytometry and annexin-V/PI staining. Ponatinib induced significant dose-dependent increases in the percentage of apoptotic cells compared with negative control at 2.5 (30.62±2.47%) and 5.0 μM (92.4±2.96%). Imatinib did not induce a significant change in the percentage of apoptotic cells at either concentration (Fig. 2C). Representative flow cytometry plots are shown in (Fig. 2D).

Ponatinib induces morphological changes and decreases number of H9c2 cardiomyoblasts. The effect of imatinib and ponatinib on cell morphology and cardiomyocyte hypertrophic markers, including cell surface area and size were assessed. Treatment with 2.5 or 5.0 μM ponatinib reduced cellular density and increased cellular detachment and cellular shrinkage compared with the Negative control (DMSO 0.1% v/v) (Fig. 3A). Imatinib treatment increased cell size, indicative of hypertrophy. Ponatinib, but not imatinib, impacted H9c2 cardiomyoblast morphology. At 2.5 μM, ponatinib cause a significant reduction in cell surface area (69.23±9.86%) compared with the negative control, indicating cell shrinkage. Furthermore, 5 μM ponatinib resulted in severe cell loss, making surface area measurement impossible. (Fig. 3A and B).

To confirm these results, flow cytometry was used to measure cell size. As expected, 2.5 and 5.0 μM ponatinib significantly reduced cell size by 37.59±14.35 and 1.26±0.22%, respectively, compared with negative control. Imatinib treatment did not induce any significant change in cell size (Fig. 3C). Representative flow cytometry plots for the cell size are shown in Fig. 3D.

Imatinib and ponatinib induce malformations in ZFEs. To confirm cardiotoxic effects of imatinib and ponatinib, ZFEs were used as an *in vivo* model. Embryos were treated with TKI and toxicity analyses were conducted by monitoring the survival and morphology for up to 72 hpf. For the 2.5 μM imatinib and ponatinib treatment, several phenotypes were observed, including edema and/or lordosis. Edema was the most common disfigurement in all ponatinib concentrations. Edema typically included cardiac malformations that disrupted the sinus rhythm of the heart. These malformations usually did not result in death of the animals. As these animals aged, they maintained their bent stature but could otherwise function normally, for example swimming and feeding. The decreased diameter of DA and posterior cardinal vein (PCV) was consistently observed in 2.5 μM imatinib and ponatinib treated embryos compared with the negative control embryos. The animals that displayed this malformation exhibited notable difficulties swimming at later time points. Dorsalization was observed in rare cases in the 10 μM ponatinib-treated embryos. Embryos exhibiting this phenotype seldom survived and failed to hatch because of the extreme nature of the deformities. Exposure to TKIs significantly

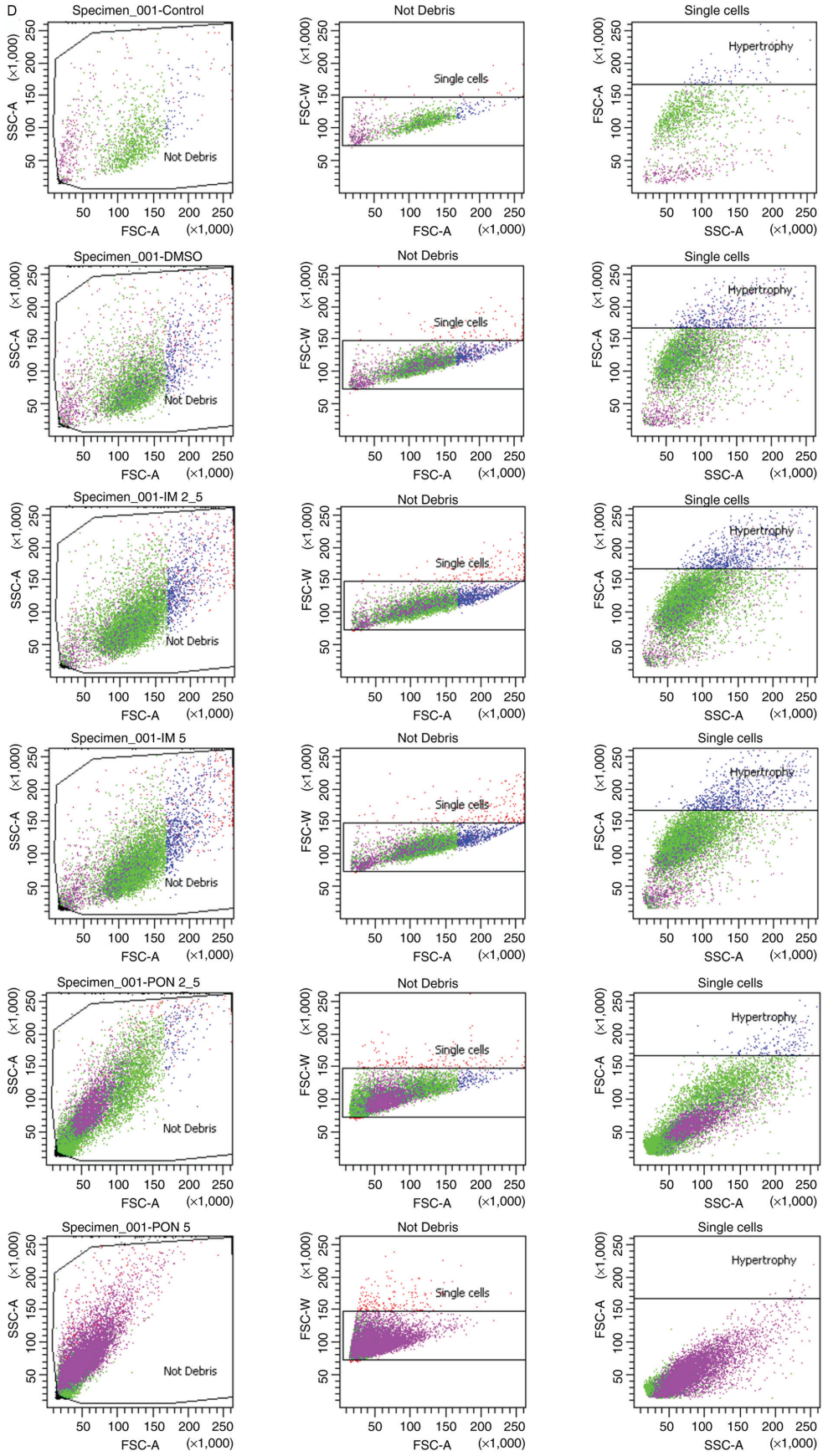

Figure 3. Effect of imatinib and ponatinib on H9c2 cardiomyoblast cell surface area. (A) Representative images and (B) quantification of H9c2 cardiomyoblasts stained with crystal violet following 24 h treatment with negative control. Images were captured with a Carl Zeiss AxioVision imaging system at a magnification of x20. (C) Cell size was analyzed using forward scatter flow cytometer analyses following 24 h treatment with negative control, imatinib or ponatinib. Values are presented and normalized as a percentage of vehicle negative control (0.5% v/v DMSO). (D) Representative forward scatter flow cytometer plots. All data are presented as mean ± SEM with 15-30 cells/group; the experiment was repeated three times. One-way ANOVA with Dunnett's post hoc test was used to compare groups. *P<0.05, ***P<0.001 and ****P<0.0001 vs. DMSO.

Table II. Dorsal aorta blood flow analysis for zebrafish embryos.

Property	Control	0.1% DMSO	2.5 μM imatinib	2.5 μM ponatinib
Blood flow velocity, μm/sec	472.00±25.30	460.40±101.30	223.80±27.40[a]	194.90±27.40[b]
Diameter, μm	15.70±2.00	14.03±2.020	9.10±1.40	9.30±6.70
Heartbeat, bpm	146.30±1.90	156.20±11.50	142.00±318.30	142.20±18.30
Sheer stress, dynes/cm^2	4.80±0.90	5.20±1.120	3.90±0.70	4.40±2.20
Cardiac output, nl/ml	5.60±1.10	4.40±1.90	0.90±0.03	1.50±1.80

Statistical analysis was performed by one-way ANOVA with Sidak's post hoc test. [a]P=0.0038 and [b]P=0.0099 vs. DMSO.

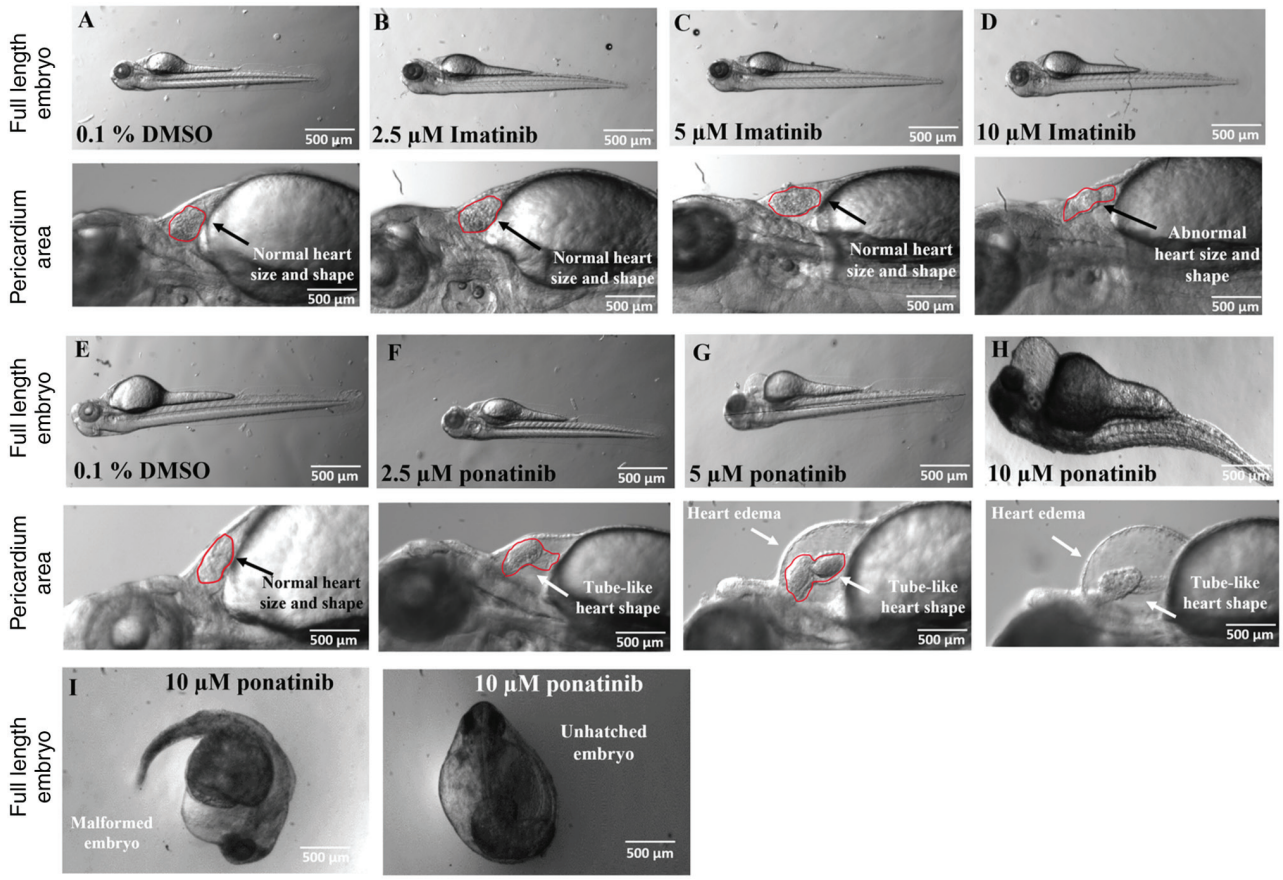

Figure 4. Effects of imatinib and ponatinib on embryo phenotypes at 72 hpf. Heart morphology was assessed under a light microscope at x100 magnification. (A) Negative control embryos treated with 0.1% v/v DMSO displayed normal heart size and shape. Imatinib treatment at (B) 2.5 and (C) 5.0 μM did not alter heart morphology. (D) Imatinib (10 μM) caused abnormal heart size and shape. (E) DMSO negative control produced normal heart structure. Ponatinib at (F) 2.5 and (G) 5.0 μM resulted in elongated, tube-like hearts and pericardial edema. (H) Single surviving embryo at 10 μM ponatinib had severe pericardial edema, a weak heart and minimal tail blood flow. (I) All embryos exposed to 10 μM ponatinib were malformed and remained did not hatch until 96 hp. A total of 20 embryos was used in each group and the experiment was repeated three times. hpf, h post-fertilization.

increased malformation rates in zebrafish embryos compared to controls treated with 1% DMSO (Fig. 4; Table II). Control embryos showed a low baseline incidence of malformations, with only 5% exhibiting edema. Imatinib impact was dose-dependent; at lower concentrations (2.5 and 5 μM), it did not significantly increase malformation rates. However, at the highest concentration (10 μM), it caused a moderate rise in edema (10%) and a substantial increase in cardiac disruptions (40%). Ponatinib demonstrated a stronger teratogenic effect than Imatinib. Even at its lowest dose (2.5 μM), Ponatinib significantly increased the prevalence of edema (20%) and cardiac disruptions (25%). The malformation rates increased as the concentration of Ponatinib rose, with 65% of embryos showing edema and 60% having cardiac issues at 5 μM. At the highest dose (10 μM), nearly all embryos displayed malformations, with 85% showing edema, 90% exhibiting lordosis, and 95% experiencing cardiac disruptions.

Imatinib and ponatinib induce developmental toxicity in ZFE. To assess the potential teratogenic effects of imatinib and ponatinib, treated embryos were visually inspected compared with the negative controls at 24, 48 and 72 hpf. As a PC for

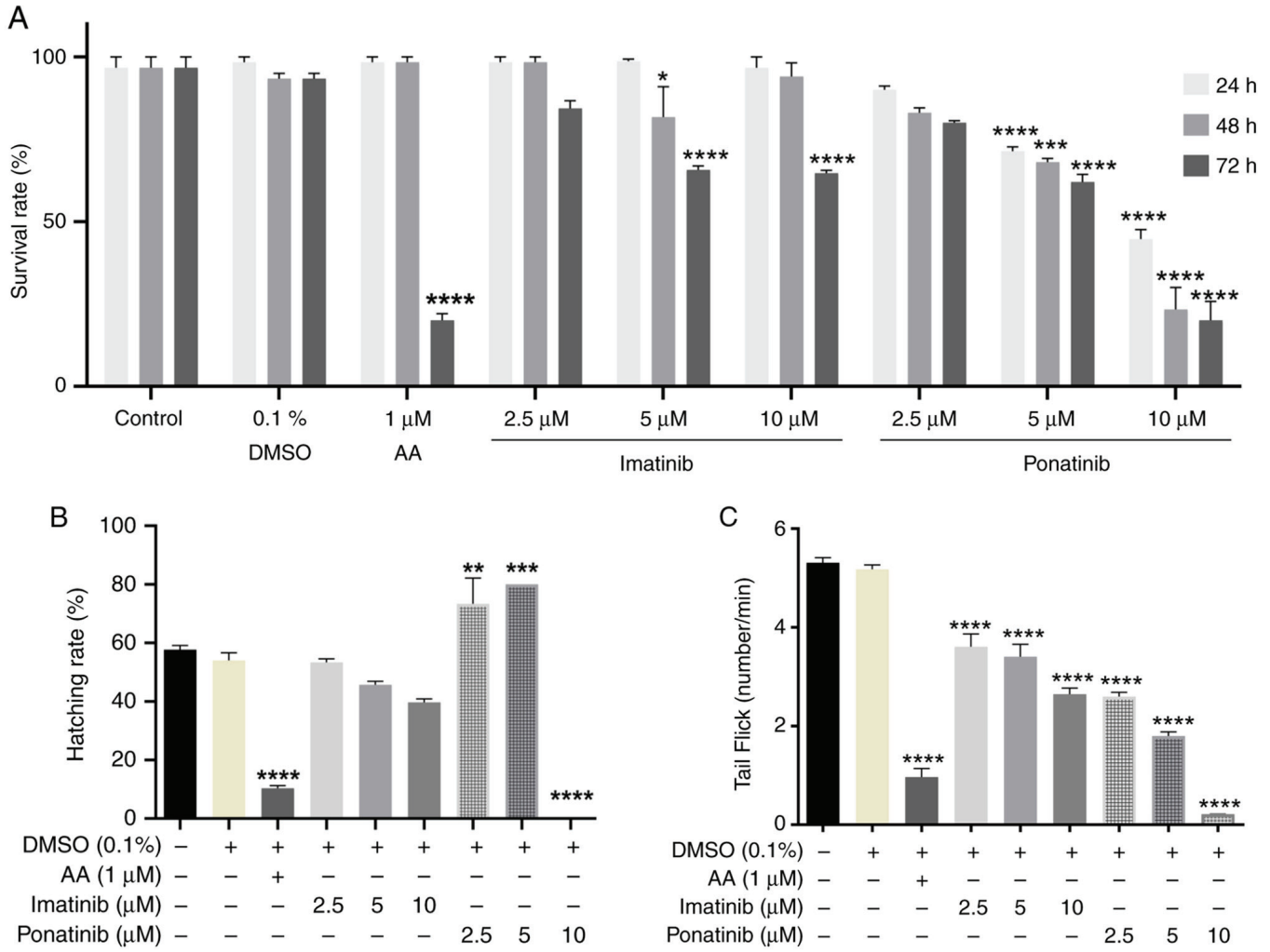

Figure 5. Effects of TKI exposure on zebrafish embryo survival, hatching and tail flicking. Zebrafish embryos were exposed to imatinib and ponatinib compared with the positive (1 μM AA) and negative control (0.1% v/v DMSO) at 24, 48 and 72 hpf. (A) Survival rate decreased in embryos exposed to Imatinib 10 μM at 72 hpf and Ponatinib 5.0, 10 μM at all timepoints compared with the negative control (0.1% v/v DMSO). Data were analyzed by two-way mixed ANOVA with Sidak's post hoc test. (B) TKI exposure significantly reduced the hatching rate at 72 hpf compared with the negative control (0.1% v/v DMSO). (C) Tail-flicking activity at 24 hpf demonstrated decreased activity in TKI-treated embryos. Data were analyzed by one-way ANOVA with Sidak's post hoc test. All data points are presented as mean ± SEM (20 embryos/group). **P<0.01, ***P<0.001 and ****P<0.0001 vs. DMSO. AA, aristolochic acid; hpf, hours post-fertilization; TKI, tyrosine kinase inhibitor.

heart failure induction, 1 μM AA was used, consistent with previous studies (38,39). Concentration-dependent decreases in survival rate and tail-flicking activity were observed in embryos treated with imatinib and ponatinib compared with the negative control (Fig. 5A and C). Ponatinib significantly affected survival rate at 5 and 10 μM concentrations. This effect began at the first day (24 h post fertilization, hpf) and persisted until 48 and 72 hpf. Both Imatinib and Ponatinib significantly affected tail flicking at all concentrations tested. However, Ponatinib exhibited a stronger inhibitory effect on both survival rate and tail flocking compared to Imatinib.

Furthermore, changes in hatching rates were observed at 48 hpf. While 2.5 and 5.0 μM ponatinib significantly increased the hatching rate compared with the control, 10 μM ponatinib significantly decreased hatching rate compared with the control. Imatinib treatment did not significantly affect hatching at any concentration. As expected, 1 μM AA significantly reduced the hatching rate compared with the negative control (0.1% v/v DMSO) (Fig. 5B).

Imatinib and ponatinib disrupt cardiac function and structure in ZFE. DA blood flow analysis demonstrated the detrimental effects of both TKIs on cardiac function. Notably, 5 and 10 μM ponatinib nearly arrested blood flow (Fig. 4I), precluding further analysis at higher concentrations. At 2.5 μM, ponatinib and imatinib significantly impaired cardiac function. Compared with negative control embryos, 2.5 μM, ponatinib and imatinib caused a significant 48% decrease in DA blood flow velocity, indicating decreased flow rate. Furthermore, 2.5 μM ponatinib and imatinib induced a significant 27% narrowing of the aorta diameter, suggesting structural abnormalities. Both TKIs caused a 73% reduction in overall flow rate compared with negative controls (Fig. 6). These findings suggest the cardiotoxic potential of both ponatinib and imatinib in developing ZFEs.

Imatinib and ponatinib upregulate cardiac failure markers in ZFE. Imatinib and ponatinib significantly increased mRNA expression of ANP and BNP compared with the

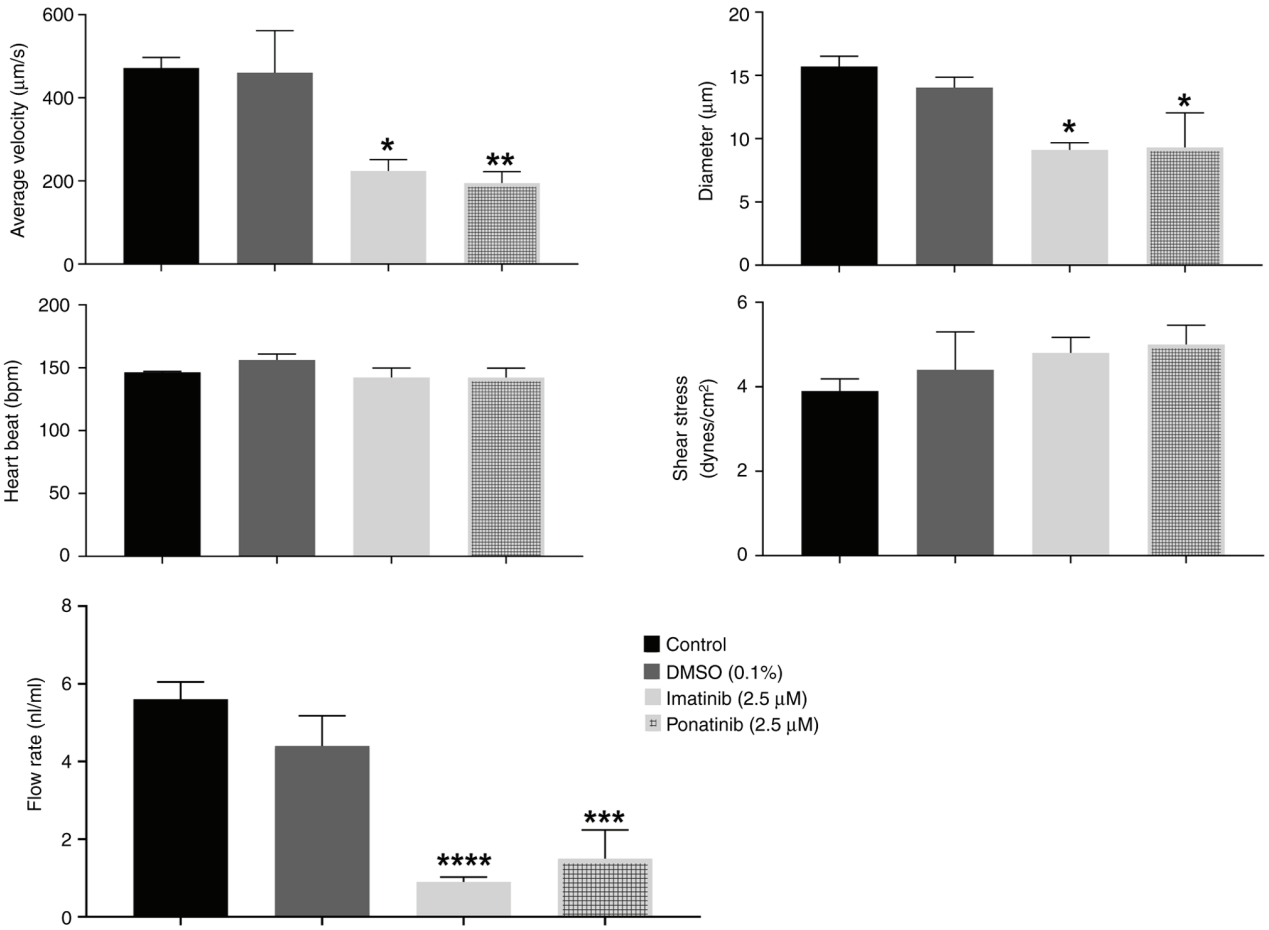

Figure 6. Cardiac function following treatment with imatinib and ponatinib. Blood flow analysis at 72 hpf in the dorsal aorta was used to assess cardiac function in embryos treated with TKIs. All data points are presented as mean ± SEM (six embryos/group); the experiment was performed three times. Statistical analysis was performed by one-way ANOVA with Sidak's post hoc test. *P<0.05, **P<0.01, ***P<0.001 and ****P<0.0001 vs. DMSO. TKI, tyrosine kinase inhibitor; hpf, hours post-fertilization; bpm, beats per minute.

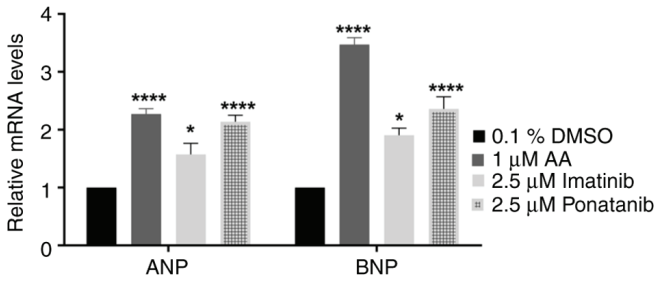

Figure 7. Gene expression changes of cardiac markers following exposure to imatinib and ponatinib. Reverse transcription-quantitative PCR analysis of ANP and BNP mRNA expression in zebrafish embryos at 72 h post-fertilization. Relative mRNA expression was calculated using the $2^{-\Delta\Delta Cq}$ method and fold-change was determined in reference to the internal reference housekeeping gene B2M. Data are presented as the mean ± SEM and experiments were performed in triplicate. Data were analyzed by two-way ANOVA followed by Tukey's post hoc test. *P<0.05 and ****P<0.0001 vs. DMSO). ANP, atrial natriuretic peptide; BNP, brain natriuretic peptide.

controls (Fig. 7). ANP and BNP are established markers of cardiac failure (40).

Ponatinib treatment significantly increased ANP and BNP mRNA expression by approximately twofold compared to the negative control. In contrast, Imatinib only caused a onefold increase in both ANP and BNP mRNA expression compared to the negative control.

These changes in gene expression mirrored those observed in embryos treated with 1 μM Aristolochic acid I (AA), a positive control for ZFE cardiotoxicity. This suggests that both TKIs (Ponatinib and Imatinib) significantly affect zebrafish embryonic development. Notably, Ponatinib's effect was comparable to the positive control (Fig. 7).

Discussion

Cardio-oncology emphasizes the importance of early detection and management of cardiotoxic effects during cancer treatment (41). These adverse effects can occur acutely, subacutely or chronically, depending on the drug and patient context (42-44). While numerous anticancer medications affect the cardiovascular system (4), multi-targeted TKIs such as imatinib and ponatinib raise concerns due to their well-established cardiotoxic potential (45-47). Novel strategies are required to mitigate TKI-induced cardiotoxicity.

Among small-molecule kinase inhibitors used for CML treatment, ponatinib carries the highest risk of cardiotoxicity, manifesting as congestive heart failure (CHF), cardiac arrhythmia and hypertension (22,48). Clinical trials report that 7% of ponatinib-treated patients experience CHF or left

ventricular dysfunction, with potentially life-threatening consequences (49-51). This heightened risk is further emphasized by the black box warning issued by the U.S. Food and Drug Administration (FDA). Black box warnings are the FDA's most stringent warnings, highlighting medications with potentially serious, long-lasting, or even fatal risks. The present study evaluated the effects of TKIs using H9c2 cells and ZF as models. Initial observations with H9c2 cells identified ponatinib more cardiotoxic than imatinib, which was confirmed in the ZF model. H9c2 cells were chosen for their established use in exploring cellular mechanisms of TKI-induced cardiotoxicity (23,25,52-56). Moreover, the ZF model offers an efficient and cost-effective means for *in vivo* toxicity assessment. Despite differences between ZF and human biology, notable genetic overlap and ability to mimic cardiotoxic effects observed in patients with cancer make them valuable tools for assessing cardiovascular toxicity associated with cancer treatment (34,56-59). Notably, zebrafish embryos offer a high-throughput screening approach but are limited to early developmental stages, it offers advantages over other *in vitro* and *in vivo* models, their rapid development, ease of use and large numbers of embryos enable quick testing of many compounds. Alternative models such as adult ZF, chick embryos and mice should be used for comprehensive analyses, including extended assessments of acute or chronic effects.

A previous study assessed the involvement of p90 ribosomal S6 kinase and autophagy in TKI-induced cardiotoxicity (60). Based on previous analyses, where cardiotoxic effects of clinically approved TKIs (Dasatinib, Nilotinib, Ponatinib) were compared and the distinct effects of Ponatinib on H9c2 cells were identified (61-64). Imatinib has well-established clinical use and relatively low cardiotoxic profile compared with other TKIs studied; therefore, ponatinib and imatinib were assessed in the present study (60,62-64).

Cytotoxic drugs such as imatinib and ponatinib affect cellular processes, including morphology, proliferation, attachment and viability (65). A particular concern is in the context of the heart, where cardiomyocyte loss serves a key role in the development of heart failure (66,67). Numerous mechanisms including autophagy, apoptosis and necrosis contribute to this loss (66,67). Moreover, pathological cardiac hypertrophy, often triggered by factors including elevated blood pressure, can lead to heart failure (68). This condition is characterized by enlarged cardiomyocytes and increased expression of natriuretic peptides such as ANP and BNP (68).

Given the link between healthy cardiomyocytes and heart failure, the potential cardiotoxic effects of imatinib and ponatinib on H9c2 cardiomyoblasts were assessed by two key indicators: Cell viability and hypertrophic response. ponatinib significantly decreased viability in H9c2 cells, demonstrating potent effect. The MTT assay indicated ~20 and ~40% reductions for 2.5 and 5 μM ponatinib, respectively, after 24 h. These findings align with other *in vitro* studies (23,24,65). While MTT assay offers a convenient and widely used method for assessing cell viability, its limitations must be acknowledged, particularly when evaluating drugs such as ponatinib that target the mitochondria (69,70). MTT assay measures formazan production, a byproduct of mitochondrial activity, as an indirect measure of cell viability (71). This can be misleading as drugs such as ponatinib primarily affect mitochondrial function without inducing substantial cell death (72). Moreover, factors beyond cell viability, such as cellular morphology and metabolic activity, influence formazan production, potentially leading to inaccuracy (71,73). Ponatinib is known to inhibit BCR-ABL TK, a protein located in the mitochondria (74). This can directly impair mitochondrial function, leading to decreased formazan production in viable cells (75). Therefore, relying solely on the MTT assay for assessing cell viability in response to ponatinib treatment may not accurately reflect the true impact on cell survival. It is key to consider using complementary assays that directly assess cell viability, such as trypan blue exclusion or flow cytometry based on viability dyes. Combining MTT assay with these alternative methods can provide a more comprehensive and reliable picture of cell viability (76), particularly when studying drugs with potential mitochondrial effects, such as Ponatinib.

Compared with MTT assay, flow cytometry showed more significant reductions in cell viability (>90% for imatinib and 35-80% for ponatinib) due to the increased sensitivity of flow cytometry (65,77). Imatinib and ponatinib induced different morphological alterations. Ponatinib caused significant shrinkage and detachment of cardiomyoblasts, while significant increase in cell viability compared with the negative control was demonstrated with 2.5 μM imatinib treatment, however, no significant changes were demonstrated at 5 μM. Cell shrinkage suggests apoptosis, while decreased surface area may indicate impaired hypertrophic response (68,78,79). These findings align with previous observations of the effect of ponatinib on Neonatal rat ventricular myocytes (80). While the adverse effects of ponatinib on cardiomyocyte morphology are concerning, further studies are needed to confirm its hypertrophic potential.

To evaluate the developmental and cardiac impacts of imatinib and ponatinib, ZFEs were treated 2.5, 5.0 and 10.0 μM imatinib or ponatinib for 72 h. To ensure minimal interference from the solvent, 0.1% DMSO was used to adhere to established minimal toxicity recommendations and The Organization for Economic Cooperation and Development guidelines (81,82). Early embryo lethality at <12 hpf was attributed to unfertilized embryos mimicking normal appearance but lacking viability. Prompt removal of these and inclusion of an untreated control group ensured that the observed lethality accurately reflected TKI exposure.

Exposure to both TKIs resulted in dose-dependent malformation, with ponatinib causing stronger effects. Notably, the consistent presence of edema across all ponatinib concentrations directly contributed to cardiac disruption and ultimately impaired long-term swimming ability, Edema is the accumulation of fluid in tissues, leading to swelling. When edema occurs in zebrafish embryos around the heart, it can physically compress the organ, impairing its ability to effectively pump blood. Additionally, the fluid from edema may carry molecules that disrupt normal signaling pathways within the heart muscle, potentially resulting in weakened contractions or abnormal heart rhythms. Decreased blood vessel diameter further emphasized the detrimental impact on cardiovascular function. The rare but severe dorsalization phenotype at 10 μM ponatinib concentrations highlighted

potential teratogenic effects. Visual inspection confirmed the teratogenic potential of both TKIs, evidenced by decreased survival and tail-flicking activity and altered hatching rates. Ponatinib exhibited a stronger inhibitory effect on hatching compared to imatinib. Ponatinib displayed a biphasic response, with low doses (2.5, 5 μM) stimulating hatching while higher concentrations (10 μM) significantly suppressed it. This suggests a dose-dependent mechanism for ponatinib's effect on hatching, distinct from that of imatinib. Notably, the AA PC further validated these results and emphasized the teratogenicity of the tested TKIs. These findings demonstrate the cardiotoxic potential of imatinib and ponatinib, extending beyond *in vitro* models and underlining potential clinical risks.

The cardiac structure and function measurement revealed that while heart rate remained consistent across TKI-treated animals, significant cardiovascular disruptions occurred even at the lowest tested concentration of 2.5 μM. Both drugs significantly decreased aortic blood flow velocity, suggesting impaired flow rate and circulation. This effect was further confirmed by the complete absence of blood flow at 10 μM ponatinib concentrations. Furthermore, the decrease in blood vessel diameter caused by ponatinib further supported its detrimental impact on the cardiovascular system. The abnormalities in heart shape and size aligned with the known cardiotoxic effects of TKIs and potentially explain these functional impairments (59). However, no significant differences in shear stress were demonstrated, suggesting that the mechanical hemodynamic effects are unlikely to be the primary driver of deformities and dysfunctions. These findings reinforce the need for further investigation into specific molecular pathways underlying TKI-induced cardiotoxicity.

Both TKIs significantly affected cardiac marker gene expression of ANP and BNP levels, Notably, Ponatinib effect was comparable to the positive control, indicating severe cardiotoxicity and potential hypertrophy. This aligns with previous studies demonstrating ponatinib-induced p90RSK phosphorylation *in vitro*, which promotes cardiomyocyte hypertrophy (60,83,84).

The present study serves as a primary screening of the cardiotoxic potential of TKIs in a ZF model. While ANP and BNP results suggest a molecular mechanism, further molecular assessment is recommended to achieve more comprehensive understanding of potential cardiotoxic effects. Future work should evaluate additional cardiomyocyte injury markers and conduct signaling pathway analysis for other markers such as Reactive Oxygen Species related genes and Vascular endothelial growth factor receptor 2 (VEGFR2). This may provide deeper knowledge of underlying mechanisms and long-term consequences associated with these drugs.

Despite their effectiveness as tyrosine kinase inhibitors (TKIs) for targeting ABL in cancers like CML, both imatinib and ponatinib present a risk of cardiotoxicity. This off-target effect likely stems from distinct pathways. Suppression of ABL by imatinib may trigger endoplasmic reticulum stress and ROS (reactive oxygen species) accumulation. This, in turn, could cripple mitochondrial function and lead to cardiotoxicity, as supported by clinical observations and damage-mimicking experiments (65,70,71). While it also promotes ROS generation and mitochondrial dysfunction, ponatinib raises additional clinical concerns like vascular complications and hypertension (16,72). Its ability to hinder blood vessel formation suggests potential off-target inhibition of VEGFR2, a receptor involved in angiogenesis (blood vessel growth) (73,74).

Despite imatinib and ponatinib sharing the mechanism of blocking RTK activity, their targeted kinases, pharmacokinetics and side effects differ. The specific pathways affected by each drug require further elucidation. Understanding the molecular mechanism is required for developing targeted interventions. Advanced tools such as transcriptome analysis and specific inhibitors should be used to identify these unique mechanisms.

In summary, the present study demonstrated that both imatinib and ponatinib exhibited distinct cardiotoxic effects, highlighting the need for further investigations of TKIs and their developmental impacts. Early detection and a comprehensive understanding of these adverse effects are crucial for improving patient outcomes and quality of life. Looking ahead, targeted delivery systems using nanoparticles offer a promising solution to minimize systemic side effects while maintaining the therapeutic efficacy of TKIs.

Building upon the established CML zebrafish model, *in vivo* assessments of these nanoparticle-based drug delivery systems can evaluate their effectiveness and safety (50). This approach holds significant promise for reducing off-target toxicity and improving the overall patient experience.

Acknowledgements

The authors would like to thank Ms Jensa Mariam Joseph, College of Pharmacy, Qatar University, Doha 2713, Qatar) for technical support.

Funding

The present study was supported by Qatar University internal funds (grant nos. QUST-BRC-SPR\2017-1 and QUUG-BRC-2017-3).

Availability of data and materials

The data generated in the present study may be requested from the corresponding author.

Authors' contributions

FM, HY and HK conceived the study. ZZ, MA and MS designed the methodology. FA, FM, FB, SS, SU and HK analyzed data. ZZ performed experiments. FA, FM, HY and HK collected data. ZZ, MS and FB wrote the manuscript. FM, HY and ZZ revised the manuscript. FM and HY supervised the study. ZZ, MA and MS performed study administration. FM, HY confirm the authenticity of the raw data. All authors have read and approved the final manuscript.

Ethics approval and consent to participate

All experiments were approved by under Qatar University Institutional Animal Care and Use Committee (approval

no. QU-IACUC 13-11/2018-REN1) and Institutional Biohazard Committee (approval no. QU-IBC-2018/057-REN2).

Patient consent for publication

Not applicable.

Competing interests

The authors declare that they have no competing interests.

References

1. Heron MP and Anderson RN: National Center for Health Statistics: Changes in the leading cause of death: recent patterns in heart disease and cancer mortality. US Department of Health and Human Services, Centers for Disease Control and Prevention. National Center for Health Statistics, Hyattsville, MD, 2016.
2. Hochhaus A and Kantarjian H: The development of dasatinib as a treatment for chronic myeloid leukemia (CML): From initial studies to application in newly diagnosed patients. J Cancer Res Clin Oncol 139: 1971-1984, 2013.
3. López-Otín C and Hunter T: The regulatory crosstalk between kinases and proteases in cancer. Nat Rev Cancer 10: 278-292, 2010.
4. Ségaliny AI, Tellez-Gabriel M, Heymann MF and Heymann D: Receptor tyrosine kinases: Characterisation, mechanism of action and therapeutic interests for bone cancers. J Bone Oncol 4: 1-12, 2015.
5. Zhang N and Li Y: Receptor tyrosine kinases: Biological functions and anticancer targeted therapy. MedComm (2020) 4: e446, 2023.
6. Chen Y, McAndrews KM and Kalluri R: Clinical and therapeutic relevance of cancer-associated fibroblasts. Nat Rev Clin Oncol 18: 792-804, 2021.
7. K Bhanumathy K, Balagopal A, Vizeacoumar FS, Vizeacoumar FJ, Freywald A and Giambra V: Protein tyrosine kinases: Their roles and their targeting in leukemia. Cancers (Basel) 13: 184, 2021.
8. Paul MK and Mukhopadhyay AK: Tyrosine kinase-role and significance in cancer. Int J Med Sci 1: 101-115, 2004.
9. Petrelli A and Giordano S: From single- to multi-target drugs in cancer therapy: When aspecificity becomes an advantage. Curr Med Chem 15: 422-432, 2008.
10. Jabbour E and Kantarjian H: Chronic myeloid leukemia: 2018 Update on diagnosis, therapy and monitoring. Am J Hematol 93: 442-459, 2018.
11. Bukowski RM: Third generation tyrosine kinase inhibitors and their development in advanced renal cell carcinoma. Front Oncol 2: 13, 2012.
12. Stasi I and Cappuzzo F: Second generation tyrosine kinase inhibitors for the treatment of metastatic non-small-cell lung cancer. Transl Respir Med 2: 2, 2014.
13. Yewale C, Baradia D, Vhora I, Patil S and Misra A: Epidermal growth factor receptor targeting in cancer: A review of trends and strategies. Biomaterials 34: 8690-8707, 2013.
14. Segaliny A, Tellez-Gabriel M, Heymann MF and Heymann D: Receptor tyrosine kinases: Characterisation, mechanism of action and therapeutic interests for bone cancers. J Bone Oncol 4: 1-12, 2015.
15. Yang Y, Li S, Wang Y, Zhao Y and Li Q: Protein tyrosine kinase inhibitor resistance in malignant tumors: Molecular mechanisms and future perspective. Signal Transduct Target Ther 7: 329, 2022.
16. Moslehi JJ: Cardiovascular toxic effects of targeted cancer therapies. N Engl J Med 375: 1457-1467, 2016.
17. Kerkelä R, Grazette L, Yacobi R, Iliescu C, Patten R, Beahm C, Walters B, Shevtsov S, Pesant S, Clubb FJ, *et al*: Cardiotoxicity of the cancer therapeutic agent imatinib mesylate. Nat Med 12: 908-916, 2006.
18. Sayegh N, Yirerong J, Agarwal N, Addison D, Fradley M, Cortes J, Weintraub NL, Sayed N, Raval G and Guha A: Cardiovascular toxicities associated with tyrosine kinase inhibitors. Curr Cardiol Rep 25: 269-280, 2023.
19. Kantarjian H, Shah NP, Hochhaus A, Cortes J, Shah S, Ayala M, Moiraghi B, Shen Z, Mayer J, Pasquini R, *et al*: Dasatinib versus imatinib in newly diagnosed chronic-phase chronic myeloid leukemia. N Engl J Med 362: 2260-2270, 2010.
20. Montani D, Bergot E, Günther S, Savale L, Bergeron A, Bourdin A, Bouvaist H, Canuet M, Pison C, Macro M, *et al*: Pulmonary arterial hypertension in patients treated by dasatinib. Circulation 125: 2128-2137, 2012.
21. Cortes JE, Kim DW, Pinilla-Ibarz J, le Coutre P, Paquette R, Chuah C, Nicolini FE, Apperley JF, Khoury HJ, Talpaz M, *et al*: A phase 2 trial of ponatinib in Philadelphia chromosome-positive leukemias. N Engl J Med 369: 1783-1796, 2013.
22. Dorer DJ, Knickerbocker RK, Baccarani M, Cortes JE, Hochhaus A, Talpaz M and Haluska FG: Impact of dose intensity of ponatinib on selected adverse events: Multivariate analyses from a pooled population of clinical trial patients. Leuk Res 48: 84-91, 2016.
23. Korashy HM, Al-Suwayeh HA, Maayah ZH, Ansari MA, Ahmad SF and Bakheet SA: Mitogen-activated protein kinases pathways mediate the sunitinib-induced hypertrophy in rat cardiomyocyte H9c2 cells. Cardiovasc Toxicol 15: 41-51, 2015.
24. Zhao Y, Xue T, Yang X, Zhu H, Ding X, Lou L, Lu W, Yang B and He Q: Autophagy plays an important role in sunitinib-mediated cell death in H9c2 cardiac muscle cells. Toxicol Appl Pharmacol 248: 20-27, 2010.
25. Will Y, Dykens JA, Nadanaciva S, Hirakawa B, Jamieson J, Marroquin LD, Hynes J, Patyna S and Jessen BA: Effect of the multitargeted tyrosine kinase inhibitors imatinib, dasatinib, sunitinib, and sorafenib on mitochondrial function in isolated rat heart mitochondria and H9c2 cells. Toxicol Sci 106: 153-161, 2008.
26. Talbert DR, Doherty KR, Trusk PB, Moran DM, Shell SA and Bacus S: A multi-parameter in vitro screen in human stem cell-derived cardiomyocytes identifies ponatinib-induced structural and functional cardiac toxicity. Toxicol Sci 143: 147-155, 2015.
27. Doherty KR, Wappel RL, Talbert DR, Trusk PB, Moran DM, Kramer JW, Brown AM, Shell SA and Bacus S: Multi-parameter in vitro toxicity testing of crizotinib, sunitinib, erlotinib, and nilotinib in human cardiomyocytes. Toxicol Appl Pharmacol 272: 245-255, 2013.
28. French KJ, Coatney RW, Renninger JP, Hu CX, Gales TL, Zhao S, Storck LM, Davis CB, McSurdy-Freed J, Chen E and Frazier KS: Differences in effects on myocardium and mitochondria by angiogenic inhibitors suggest separate mechanisms of cardiotoxicity. Toxicol Pathol 38: 691-702, 2010.
29. Pembrey RS, Marshall KC and Schneider RP: Cell surface analysis techniques: What do cell preparation protocols do to cell surface properties? Appl Environ Microbiol 65: 2877-2894, 1999.
30. Prabhu KS, Siveen KS, Kuttikrishnan S, Iskandarani A, Tsakou M, Achkar IW, Therachiyil L, Krishnankutty R, Parray A, Kulinski M, *et al*: Targeting of X-linked inhibitor of apoptosis protein and PI3-kinase/AKT signaling by embelin suppresses growth of leukemic cells. PLoS One 12: e0180895, 2017.
31. Khan AQ, Siveen KS, Prabhu KS, Kuttikrishnan S, Akhtar S, Shaar A, Raza A, Mraiche F, Dermime S and Uddin S: Curcumin-mediated degradation of S-phase kinase protein 2 induces cytotoxic effects in human papillomavirus-positive and negative squamous carcinoma cells. Front Oncol 8: 399, 2018.
32. Westerfield M: The zebrafish book: A guide for the laboratory use of zebrafish (Danio rerio). 4th edition. University of Oregon Press, Eugene, 2000. http://zfin. org/zf_info/zfbook/zfbk. html.
33. Kimmel CB, Ballard WW, Kimmel SR, Ullmann B and Schilling TF: Stages of embryonic development of the zebrafish. Dev Dyn 203: 253-310, 1995.
34. Benslimane FM, Zakaria ZZ, Shurbaji S, Abdelrasool MKA, Al-Badr MAHI, Al Absi ESK and Yalcin HC: Cardiac function and blood flow hemodynamics assessment of zebrafish (Danio rerio) using high-speed video microscopy. Micron 136: 102876, 2020.
35. Yalcin HC, Amindari A, Butcher JT, Althani A and Yacoub M: Heart function and hemodynamics analysis for zebrafish embryos. Dev Dyn 246: 868-880, 2017.
36. Benslimane FM, Alser M, Zakaria ZZ, Sharma A, Abdelrahman HA and Yalcin HC: Adaptation of a mice doppler echocardiography platform to measure cardiac flow velocities for embryonic chicken and adult zebrafish. Front Bioeng Biotechnol 7: 96, 2019.
37. Rao X, Huang X, Zhou Z and Lin X: An improvement of the 2ˆ(-delta delta CT) method for quantitative real-time polymerase chain reaction data analysis. Biostat Bioinforma Biomath 3: 71-85, 2013.
38. Huang CC, Chen PC, Huang CW and Yu J: Aristolochic acid induces heart failure in zebrafish embryos that is mediated by inflammation. Toxicol Sci 100: 486-494, 2007.
39. Narumanchi S, Wang H, Perttunen S, Tikkanen I, Lakkisto P and Paavola J: Zebrafish heart failure models. Front Cell Dev Biol 9: 662583, 2021.

40. Januzzi JL Jr: Natriuretic peptides as biomarkers in heart failure. J Investig Med 61: 950-955, 2013.
41. Wickramasinghe CD, Nguyen KL, Watson KE, Vorobiof G and Yang EH: Concepts in cardio-oncology: Definitions, mechanisms, diagnosis and treatment strategies of cancer therapy-induced cardiotoxicity. Future Oncol 12: 855-870, 2016.
42. Dolci A, Dominici R, Cardinale D, Sandri MT and Panteghini M: Biochemical markers for prediction of chemotherapy-induced cardiotoxicity: Systematic review of the literature and recommendations for use. Am J Clin Pathol 130: 688-695, 2008.
43. Pai VB and Nahata MC: Cardiotoxicity of chemotherapeutic agents: Incidence, treatment and prevention. Drug Saf 22: 263-302, 2000.
44. Albini A, Pennesi G, Donatelli F, Cammarota R, De Flora S and Noonan DM: Cardiotoxicity of anticancer drugs: The need for cardio-oncology and cardio-oncological prevention. J Natl Cancer Inst 102: 14-25, 2010.
45. Sheng CC, Amiri-Kordestani L, Palmby T, Force T, Hong CC, Wu JC, Croce K, Kim G and Moslehi J: 21st Century cardio-oncology: Identifying cardiac safety signals in the era of personalized medicine. JACC Basic Transl Sci 1: 386-398, 2016.
46. Cortes JE, Kim DW, Pinilla-Ibarz J, Le Coutre P, Paquette R, Chuah C, Nicolini FE, Apperley JF, Khoury HJ, Talpaz M, *et al*: Long-term follow-up of ponatinib efficacy and safety in the phase 2 PACE trial. Blood 124: 3135, 2014.
47. Sayed-Ahmed MM, Alrufaiq BI, Alrikabi A, Abdullah ML, Hafez MM and Al-Shabanah OA: Carnitine supplementation attenuates sunitinib-induced inhibition of AMP-activated protein kinase downstream signals in cardiac tissues. Cardiovasc Toxicol 19: 344-356, 2019.
48. Jin Y, Xu Z, Yan H, He Q, Yang X and Luo P: A comprehensive review of clinical cardiotoxicity incidence of FDA-approved small-molecule kinase inhibitors. Front Pharmacol 11: 891, 2020.
49. Moslehi JJ and Deininger M: Tyrosine kinase inhibitor-associated cardiovascular toxicity in chronic myeloid leukemia. J Clin Oncol 33: 4210-4218, 2015.
50. Shah RR and Morganroth J: Update on cardiovascular safety of tyrosine kinase inhibitors: With a special focus on QT interval, left ventricular dysfunction and overall risk/benefit. Drug Saf 38: 693-710, 2015.
51. Cortes JE, Kim DW, Pinilla-Ibarz J, le Coutre P, Paquette R, Chuah C, Nicolini FE, Apperley JF, Khoury HJ, Talpaz M, *et al*: Long-term follow-up of ponatinib efficacy and safety in the phase 2 PACE trial. Blood 124: 3135, 2014.
52. Zordoky BN and El-Kadi AOS: H9c2 cell line is a valuable in vitro model to study the drug metabolizing enzymes in the heart. J Pharmacol Toxicol Methods 56: 317-322, 2007.
53. Watkins SJ, Borthwick GM and Arthur HM: The H9C2 cell line and primary neonatal cardiomyocyte cells show similar hypertrophic responses in vitro. In Vitro Cell Dev Biol Anim 47: 125-131, 2011.
54. Witek P, Korga A, Burdan F, Ostrowska M, Nosowska B, Iwan M and Dudka J: The effect of a number of H9C2 rat cardiomyocytes passage on repeatability of cytotoxicity study results. Cytotechnology 68: 2407-2415, 2016.
55. Kobuszewska A, Tomecka E, Zukowski K, Jastrzebska E, Chudy M, Dybko A, Renaud P and Brzozka Z: Heart-on-a-Chip: An investigation of the influence of static and perfusion conditions on cardiac (H9C2) cell proliferation, morphology, and alignment. SLAS Technol 22: 536-546, 2017.
56. Bouleftour W, Mery B, Rowinski E, Rivier C, Daguenet E and Magne N: Cardio-oncology preclinical models: A comprehensive review. Anticancer Res 41: 5355-5364, 2021.
57. Khan FR and Alhewairini SS: Zebrafish (Danio rerio) as a model organism. Curr Trends Cancer manage 27: 3-18, 2018.
58. Lane S, More LA and Asnani A: Zebrafish models of cancer therapy-induced cardiovascular toxicity. J Cardiovasc Dev Dis 8: 8, 2021.
59. Al-Thani HF, Shurbaji S, Zakaria ZZ, Hasan MH, Goracinova K, Korashy HM and Yalcin HC: Reduced cardiotoxicity of ponatinib-loaded PLGA-PEG-PLGA nanoparticles in zebrafish xenograft model. Materials (Basel) 15: 3960, 2022.
60. Suleiman M: The role of P90 ribosomal S6 kinase and autophagy in sunitinib and ponatinib-induced cardiotoxicity, 2019.
61. Lekes D, Szadvari I, Krizanova O, Lopusna K, Rezuchova I, Novakova M, Novakova Z, Parak T and Babula P: Nilotinib induces ER stress and cell death in H9c2 cells. Physiol Res 65 (Suppl 4): S505-S514, 2016.
62. Wang H, Wang Y, Li J, He Z, Boswell SA, Chung M, You F and Han S: Three tyrosine kinase inhibitors cause cardiotoxicity by inducing endoplasmic reticulum stress and inflammation in cardiomyocytes. BMC Med 21: 147, 2023.
63. Lamore SD, Kohnken RA, Peters MF and Kolaja KL: Cardiovascular toxicity induced by kinase inhibitors: Mechanisms and preclinical approaches. Chem Res Toxicol 33: 125-136, 2020.
64. Sun S, Qin J, Liao W, Gao X, Shang Z, Luo D and Xiong S: Mitochondrial dysfunction in cardiotoxicity induced by BCR-ABL1 tyrosine kinase inhibitors-underlying mechanisms, detection, potential therapies. Cardiovasc Toxicol 23: 233-254, 2023.
65. Méry B, Guy JB, Vallard A, Espenel S, Ardail D, Rodriguez-Lafrasse C, Rancoule C and Magné N: In vitro cell death determination for drug discovery: A landscape review of real issues. J Cell Death 10: 1179670717691251, 2017.
66. Yussman MG, Toyokawa T, Odley A, Lynch RA, Wu G, Colbert MC, Aronow BJ, Lorenz JN and Dorn GW II: Mitochondrial death protein Nix is induced in cardiac hypertrophy and triggers apoptotic cardiomyopathy. Nat Med 8: 725-730, 2002.
67. Kostin S, Pool L, Elsässer A, Hein S, Drexler HC, Arnon E, Hayakawa Y, Zimmermann R, Bauer E, Klövekorn WP and Schaper J: Myocytes die by multiple mechanisms in failing human hearts. Circ Res 92: 715-724, 2003.
68. Tham YK, Bernardo BC, Ooi JY, Weeks KL and McMullen JR: Pathophysiology of cardiac hypertrophy and heart failure: Signaling pathways and novel therapeutic targets. Arch Toxicol 89: 1401-1438, 2015.
69. Ghasemi M, Turnbull T, Sebastian S and Kempson I: The MTT assay: Utility, limitations, pitfalls, and interpretation in bulk and single-cell analysis. Int J Mol Sci 22: 12827, 2021.
70. Rai Y, Pathak R, Kumari N, Sah DK, Pandey S, Kalra N, Soni R, Dwarakanath BS and Bhatt AN: Mitochondrial biogenesis and metabolic hyperactivation limits the application of MTT assay in the estimation of radiation induced growth inhibition. Sci Rep 8: 1531, 2018.
71. van Meerloo J, Kaspers GJ and Cloos J: Cell sensitivity assays: The MTT assay. Methods Mol Biol 731: 237-245, 2011.
72. Yu T, Cao J, Alaa Eddine M, Moustafa M, Mock A, Erkut C, Abdollahi A, Warta R, Unterberg A, Herold-Mende C and Jungwirth G: Receptor-tyrosine kinase inhibitor ponatinib inhibits meningioma growth in vitro and in vivo. Cancers (Basel) 13: 5898, 2021.
73. Ghasemi M, Liang S, Luu QM and Kempson I: The MTT assay: A method for error minimization and interpretation in measuring cytotoxicity and estimating cell viability. Methods Mol Biol 2644: 15-33, 2023.
74. Gustafson D, Fish JE, Lipton JH and Aghel N: Mechanisms of cardiovascular toxicity of BCR-ABL1 tyrosine kinase inhibitors in chronic myelogenous leukemia. Curr Hematol Malig Rep 15: 20-30, 2020.
75. Loren CP, Aslan JE, Rigg RA, Nowak MS, Healy LD, Gruber A, Druker BJ and McCarty OJ: The BCR-ABL inhibitor ponatinib inhibits platelet immunoreceptor tyrosine-based activation motif (ITAM) signaling, platelet activation and aggregate formation under shear. Thromb Res 135: 155-160, 2015.
76. Menyhárt O, Harami-Papp H, Sukumar S, Schäfer R, Magnani L, de Barrios O and Győrffy B: Guidelines for the selection of functional assays to evaluate the hallmarks of cancer. Biochim Biophys Acta 1866: 300-319, 2016.
77. Wang X, Xia Y, Liu L, Liu M, Gu N, Guang H and Zhang F: Comparison of MTT assay, flow cytometry, and RT-PCR in the evaluation of cytotoxicity of five prosthodontic materials. J Biomed Mater Res B Appl Biomater 95: 357-364, 2010.
78. Yurinskaya V, Aksenov N, Moshkov A, Model M, Goryachaya T and Vereninov A: A comparative study of U937 cell size changes during apoptosis initiation by flow cytometry, light scattering, water assay and electronic sizing. Apoptosis 22: 1287-1295, 2017.
79. Chen L, Zhao L, Samanta A, Mahmoudi SM, Buehler T, Cantilena A, Vincent RJ, Girgis M, Breeden J, Asante S, *et al*: STAT3 balances myocyte hypertrophy vis-à-vis autophagy in response to Angiotensin II by modulating the AMPKα/mTOR axis. PLoS One 12: e0179835, 2017.
80. Hasinoff BB, Patel D and Wu X: The myocyte-damaging effects of the BCR-ABL1-targeted tyrosine kinase inhibitors increase with potency and decrease with specificity. Cardiovasc Toxicol 17: 297-306, 2017.

81. Hoyberghs J, Bars C, Ayuso M, Van Ginneken C, Foubert K and Van Cruchten S: DMSO concentrations up to 1% are safe to be used in the zebrafish embryo developmental toxicity assay. Front Toxicol 3: 804033, 2021.
82. OECD: OECD guidelines for the testing of chemicals. Oecd, 1994.
83. Jaballah M, Mohamed IA, Alemrayat B, Al-Sulaiti F, Mlih M and Mraiche F: Na+/H+ exchanger isoform 1 induced cardiomyocyte hypertrophy involves activation of p90 ribosomal s6 kinase. PLoS One 10: e0122230, 2015.
84. Yamaguchi N, Chakraborty A, Pasek DA, Molkentin JD and Meissner G: Dysfunctional ryanodine receptor and cardiac hypertrophy: Role of signaling molecules. Am J Physiol Heart Circ Physiol 300: H2187-H2195, 2011.